

**Comparison of Limit Load Solutions with Results of Collapse
Tests of Perforated Plates with a Triangular Penetration Pattern**

D. P. Jones
J. L. Gordon

DE-AC11-98PN38206

NOTICE

This report was prepared as an account of work sponsored by the United States Government. Neither the United States, nor the United States Department of Energy, nor any of their employees, nor any of their contractors, subcontractors, or their employees, makes any warranty, express or implied, or assumes any legal liability or responsibility for the accuracy, completeness or usefulness of any information, apparatus, product or process disclosed, or represents that its use would not infringe privately owned rights.

BETTIS ATOMIC POWER LABORATORY

WEST MIFFLIN, PENNSYLVANIA 15122-0079

Operated for the U.S. Department of Energy
by Bechtel Bettis, Inc.

Comparison of Limit Load Solutions with Results of Collapse Tests of Perforated Plates with a Triangular Penetration Pattern

D. P. Jones* and J. L. Gordon*

Bechtel Bettis, Inc
West Mifflin, PA 15122-0079

*Member, ASME

ABSTRACT

Limit load solutions obtained by elastic-perfectly plastic finite element analysis (EPP-FEA) are compared to results of tests of low-alloy steel perforated plate geometries loaded to full plastic collapse. Results are given for two plastic-collapse tests of flat circular disks with circular penetrations arranged in a triangular pattern and drilled normal to the surface of the plate. The ligament efficiency (minimum distance between holes divided by the distance between the centers of the holes) of the pattern is 0.32 and the plate thickness is 2.39 inches (60.7 mm). The tests were designed so that a transverse load generated plastic collapse in the outer row of penetrations due to a combination of transverse shear and in-plane bending. Limit-load solutions were obtained using EPP-FEA with small-strain, small-deflection linear geometry assumptions. Two FEA models are used: one where the perforated region is modeled using an equivalent solid plate (EQS) representation and another where each hole is explicitly modeled by FEA. The results presented in this paper demonstrate that the deformation patterns produced by the EPP-FEA solutions match exactly with the deformation patterns produced by the test. The EQS-EPP FEA solution is about 15% lower than the explicit-hole EPP-FEA solution. Using one-third the actual ultimate strength of the material as the strength parameter in the limit load calculation produces a calculated limit load that is greater than

a factor of three less than the mean measured plastic-collapse load obtained in the tests. This paper adds to the qualification of the use of limit-load solutions obtained using small-strain, small deflection EPP-FEA programs for the calculation of the limit load for perforated plates.

NOMENCLATURE

P	Distance between penetration centers, mm
h	Minimum ligament width, mm
$\mu = h/P$	Ligament efficiency
S_{ult}	Ultimate strength of the material, MPa
S_y	Yield stress, MPa
S_m	Material strength allowable, $S_{ult}/3$, MPa
EQS	Equivalent solid
EPP	Elastic perfectly plastic
R_i^*	$R_i - (P - h)/4$
R_o^*	$R_o + (P - h)/4$
R_i	Radius to center of inner-most penetration
R_o	Radius to center of outer-most penetration
t	Thickness of plate, mm

Introduction

Advances in computer technology have made limit load computations practical for a large number of pressure vessel components. One such component for which limit load technology can be particularly attractive is for flat perforated plates used as tubesheets in heat exchanger equipment. Justifying a reduction of just a few inches in thickness of a steam generator tubesheet can result in considerable cost savings since the reduced thickness is translated into savings in hole drilling operations.

However, even with the advances in computer technology, the use of elastic-plastic finite element analysis [EPP-FEA] to analyze a tubesheet with 10,000 holes is daunting. For this reason, considerable effort has been placed into the development of elastic-perfectly-plastic equivalent solid plate [EPP-EQS] methods. Such methods are analogous to the standard elastic EQS plate method used in Section III of the ASME Code [1] for the design of perforated plates. Elastic EQS methods are well documented by Slot [2]. References [3 through 8] document the advances in EPP-EQS methods for calculating limit loads of perforated plates.

This paper presents qualification of general EPP-FEA and EQS-EPP-FEA methods to conservatively compute the limit load of perforated plates. Qualification is by comparison of calculated limit load solutions to test results of plastic-collapse loads for a perforated plate.

The test sample is a flat perforated plate loaded in the direction parallel to the axis of the penetrations until plastic collapse is achieved. The holes are placed in a triangular pattern with ligament efficiency [h/P] of 0.32. The pitch of the pattern is 0.75 inch (19.1 mm) and the plate is 2.39 inches (60.7 mm) thick. Each plate has five rows of penetrations for a total of 414 penetrations. Two plates are tested with load deflection curves recorded to complete plastic collapse.

The calculated limit load is obtained by two methods: by the EPP-EQS method and by EPP-FEA where each penetration is modeled explicitly.

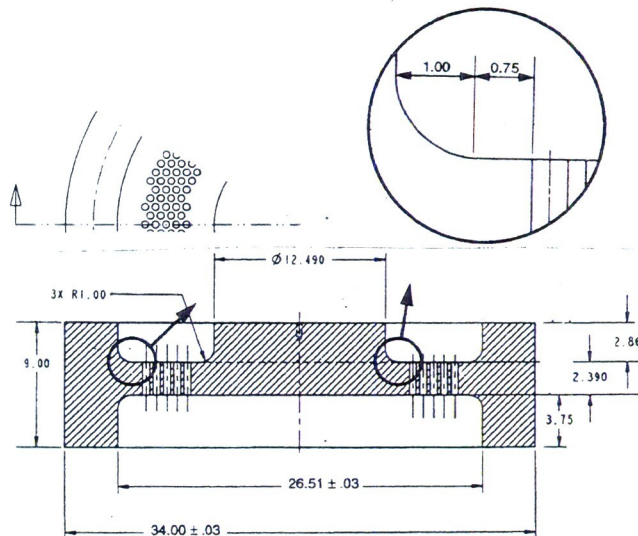
The test load-to-plastic collapse is compared with the calculated loads to qualify the method.

Test

One of the limiting locations of a steam-generator shell-to-tubesheet juncture is at the perforated-solid material interface. Typically this row of penetrations is loaded in a combination of in-plane bending and out-of-plane shear. A test was designed to provide a critical assessment of the analytical methods to predict this failure mode.

The test plate is shown in Figure 1. The outside diameter of test sample is 34 inches (863.6 mm) and the inside hub is 12.49 inches (317.5 mm) in diameter. There are five rows of holes on an annulus ring of 16.5 inches (419 mm) inside diameter and 22.5 inches (571.5 mm) outside diameter. The plates are made of low-alloy steel.

Figure 1. Test plate. (Dimensions in inches.)



Two plates were tested in this program. The plates were loaded in a hydraulic press capable of exerting a 5,000 kip load on the inner hub. Strain gage measurements, transverse displacement, and a digital image mapping technique to measure strains in the ligaments were used. Since the purpose of this paper is to qualify the limit load technology, only the load-deflection data and location of the collapse is reported here. Qualification of calculated strain is outside the scope of this study.

The tests were conducted at the Fritz Engineering Laboratory at Lehigh University in Bethlehem, Pennsylvania. The test machine is shown in Figures 2 and 3. The test machine is calibrated yearly to ASTM E-4 requirements and the dual load cells are calibrated to record loads to \pm 100 pounds up to 4,500 kips.

Figure 2. Testing machine.

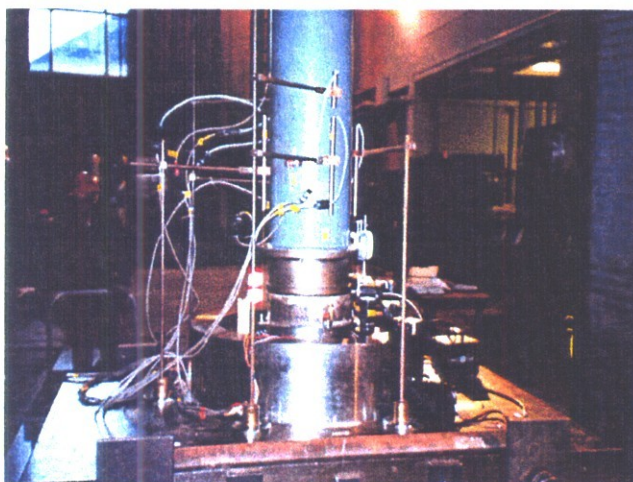
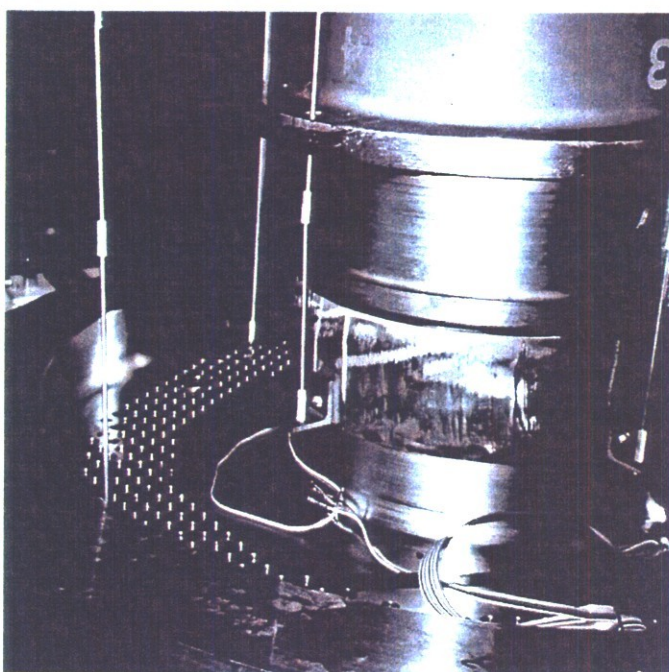


Figure 3. Arrangement of LVDTs.



The displacements were measured using four Marco Sensors DC-750 Linear Variable Differential Transformer (LVDTs) linear position sensors. These LVDTs have 0.25% non-linearity resolutions. Two-inch LVDTs provided displacement data throughout the test into the plastic range. The LVDTs were arranged at approximately 90° intervals on the inside hub of the specimen. This is the location of the maximum displacement as the hub acts as a nearly rigid body simply transferring the load to the perforated region. Figure 3 shows the arrangement of the LVDTs.

The test machine was fixed with two platen-leveling plates to minimize misalignments. By making four alignment measurements approximately 90 degrees apart, misalignment is kept to a minimum.

Tensile data was taken for the plate material. Elastic properties and average results of nine tensile tests of the test material are shown in Table 1. A material allowable (S_m) is given as $S_{ult}/3$.

Table 1. Material Properties

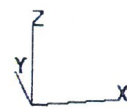
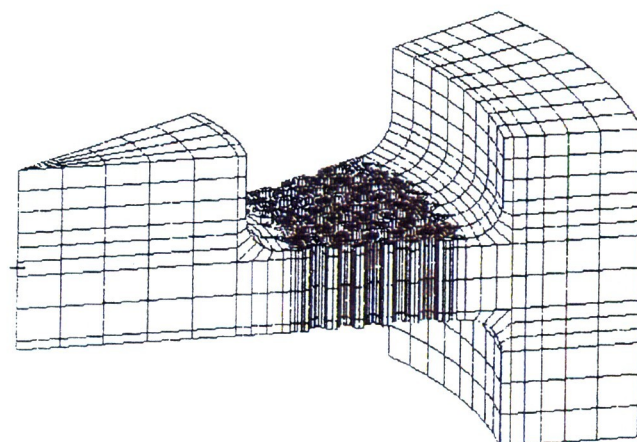
Young's Modulus [psi]	Poisson's Ratio	0.2% Yield Strength Avg of 9 [psi]	Ultimate Strength Avg of 9 S_{ult} [psi]	$S_{ult/3}$ Material Allowable S_m [psi]
27.7×10^6	0.3	95,081	114,091	38,030

In order to qualify limit load calculations, only the load-displacement comparisons are provided. Qualitative comparisons are made with the visual observations in order to ascertain that the computations are simulating the same location and mode of failure as observed in the test.

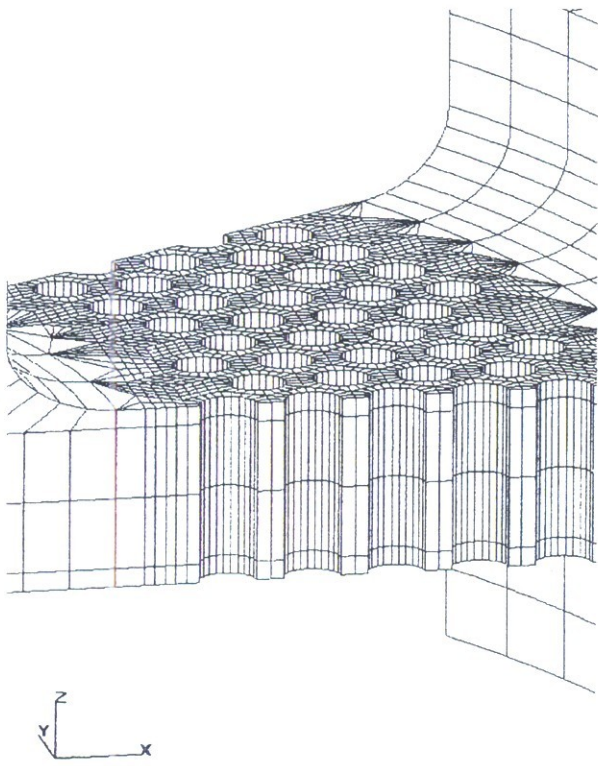
EPP-FEA Model

The most straight-forward use of FEA is to simply model each penetration in the structure and use EPP-FEA to calculate the limit load. This is called the explicit-hole EPP-FEA solution here. A model using 30 degree symmetry is shown in Figures 4 and 5.

The ABAQUS [9] FEA program was used. The model has 44,784 20-node, reduced integration elements with 216,486 nodes. The load is applied over a two inch (50.8 mm) annulus region (A-B in Figure 6) to simulate the load ram contact with the loading hub. The specimen is assumed to be in contact with the lower platen over a one inch (25.4 mm) annulus (C-D in Figure 6). The lift-off of the specimen was measured during the test and none was observed. Larger and smaller load and reaction areas were tried and no difference was observed in the calculated limit load.

Figure 4. Explicit FEA model.

As discussed by Kalnins and Updike [10], linear geometry options were used to calculate a limit load. The finite element models were run in ABAQUS until a very small increase in load (100 psi increments over the applied load annulus area) resulted in a very large increase in deflection.

Figure 5. Ligament region.

EPP-EQS Model

The EPP-EQS model is shown in Figure 6. This model is an axisymmetric FEA model with 180 elements and 621 nodes. The ABAQUS eight-node reduced integration axisymmetric element was used in this FEA model. The extent of the EQS region is termed R^* in the ASME Code [1]. The outside and inside radius of the perforated region is set at

$$R_o^* = R_o + (P - h)/4$$

$$R_i^* = R_i - (P - h)/4$$

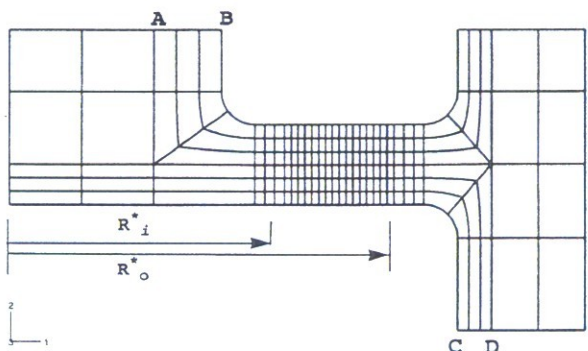
Where R_o is the distance to the center of the outer-most hole and R_i is the radius to the center of the inner-most hole. Table 2 provides the values used for these models.

Rather coarse FEA meshes are used in both the 2D and 3D models since the objective of these analyses is to predict limit loads. Kalnins and Updike [10] discuss the role of FEA mesh refinement and accuracy of calculated limit loads.

Table 2. EQS geometry parameters.

R_o	R_o^*	R_i	R_i^*
11.25 inches (285.8 mm)	11.378 inches (289 mm)	8.250 inches (209.6 mm)	8.122 inches (206.3 mm)

The EPP-EQS limit load for this model is obtained in ABAQUS using a user defined material model (called a UMAT in ABAQUS) that is based on the EPP flow theory developed by Gordon and Jones [5] for the fourth-order collapse function to represent the perforated region. A new UMAT has been developed by Gordon and Jones [8] using a sixth order collapse function in place of the fourth order function. Results are given in this paper for both the sixth order UMAT (called UMAT6 here) and the fourth-order UMAT (called UMAT4 here). The same base material properties and boundary conditions are used in both the EPP-EQS model and the explicit FEA model.

Figure 6. Axisymmetric EPP-EQS FEA model.

OBSERVATIONS

The test plates first failed by plastic collapse at the inner row of penetrations. This initial failure was accompanied by very large deformation at the outer row of penetrations. Figure 7 shows the deformed shape from the test. The deformed shape from the explicit FEA solution is shown in Figure 8 and from the EPP-EQS solution in Figure 9. The calculated and test deformed shapes are remarkably similar indicating the FEA method is computing the correct failure mode. There is virtually no difference between the deformed shape using the fourth order or the sixth order collapse function.

The load-deflection data from the two tests are compared to the load-deflection curves calculated by the EPP-FEA programs in Figure 10. The load is divided by a factor (PLL) that represents the shear-out load at the radius at which the failure occurred. In this case, failure occurred at R_i^* and a load factor of $PLL = 2\pi\mu S_y t R_i^*$ is used to non-dimensionalize the load.

The EPP-FEA calculated load-deflection curves are of the same shape. Both the sixth order and fourth order UMAT predictions are within 15.3% of the collapse load calculated using the explicit FEA so only one EPP-EQS-FEA result is plotted.

Table 3 compares the calculated versus test collapse loads. The collapse load is calculated by the FEA models using a yield strength analogous to the ASME Code allowable of the lesser of $2 S_y/3$ or $S_{ult}/3$. The material allowable is thus $S_{ult}/3$ or 38,030 psi (262.2 MPa). The calculated collapse load from the explicit EPP-FEA model is a factor of 3.24 below the average of the test loads while the EPP-EQS solutions are 3.81 below the test load for UMAT4 and 3.69 below the test load for UMAT6. The ASME Code requires at least a factor of 3.0 against plastic collapse and burst. These three methods comply with those requirements. If the plates were made of a material that is limited by $2 S_y/3$, the factor against plastic collapse load would be greater than a factor of 3 because of strain hardening. However, a test using a material with appropriate properties should be run before such conclusions can be made.

DISCUSSION

Comparing the EPP-EQS model with the explicit FEA model demonstrates the modeling advantage of the EQS method. The calculated results for the UMAT4 and UMAT6 methods also support use of the EPP-EQS method for limit load calculations of perforated structures.

In addition to the obvious modeling advantage, there is also a big difference between computer run times for the EQS-EPP and explicit-hole EPP-FEA solutions. The explicit FEA solution took several hours on the Compaq Alpha supercomputer while the EPP-EQS solutions take about two minutes on an SGI workstation.

Comparing the deformed geometries from the test with the explicit FEA model demonstrates that the structure collapsed due to shear and bending at the inner perforated-to-solid rim intersection (or at R_i^* as discussed in the ASME Code [1]). The EPP-EQS methods also show that the plate collapse is at the inner row of penetrations. Significant deformation is also present in the outer row of penetrations. These deformation patterns are exactly what was observed in the test samples. The fourth and sixth order collapse functions use the same approximations to model the shear collapse behavior transverse to the plane of the plate, i.e., the in-plane and out-of-plane response is uncoupled. Accordingly, there is very little difference between the UMAT4 and UMAT6 results for this test model. Larger differences would be expected if the perforated region were to fail due to in-plane shear for example.

Figure 7. Deformed shape from test.

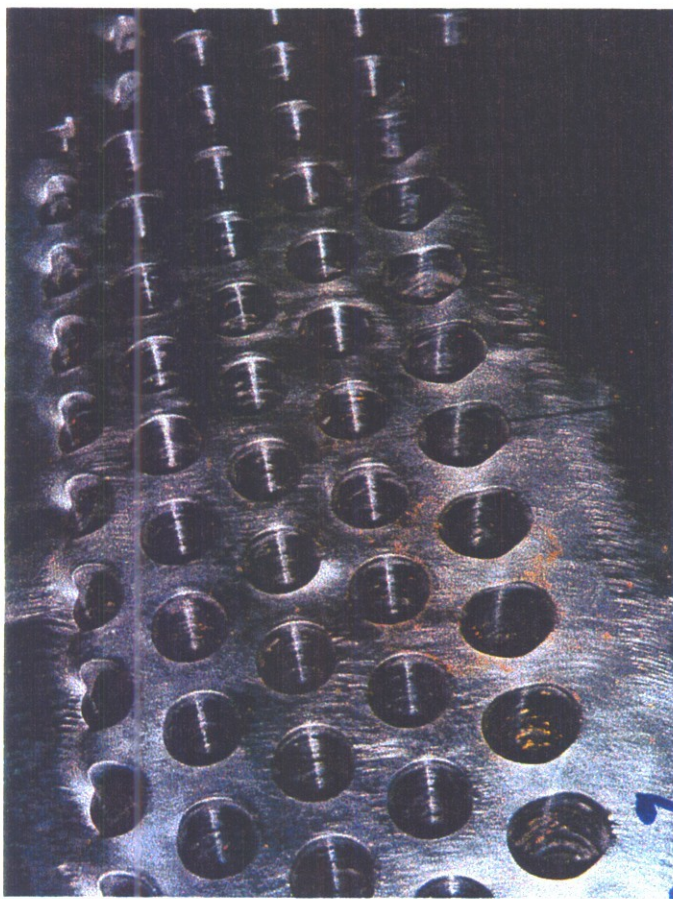
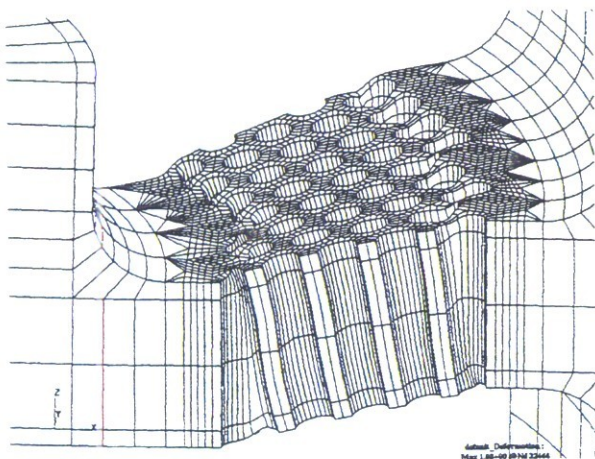


Figure 8. Deformed shape from explicit-FEA.

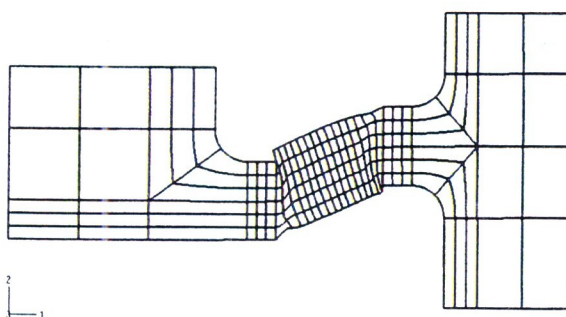


CONCLUSIONS

The finite element analysis method to calculate limit load has been qualified by comparing calculated limit loads to measured collapse loads from testing thick perforated plates containing a triangular penetration pattern with ligament efficiency of 0.32. Finite element models that explicitly represent each penetration are used as well as equivalent solid models that incorporate the collapse mechanisms of the perforated region by higher-order collapse functions. Based on this work, the following conclusions are drawn:

- The FEA method is qualified for calculating limit load for circular perforated flat plates. Both the explicit and equivalent solid FEA methods use small-deflection, small-strain assumptions and reduced integration elements with the consistent tangent modulus method of plasticity.
- The calculated collapse loads are more than a factor of three below the measured collapse loads when using a material allowable of $S_{ul}/3$ as defined in the ASME Code.
- The deformation shapes from both the explicit and equivalent FEA methods confirm that the FEA method models the correct failure mechanism for collapse of perforated materials failing in transverse shear.
- The fourth-order and sixth-order collapse functions produce accurate and conservative equivalent solid plate limit load methods for FEA applications.
- The equivalent solid plate method is a viable and efficient method of modeling perforated plates for the purpose of calculating limit load.

Figure 9. Deformed shape from EPP-EQS FEA model.



ACKNOWLEDGEMENTS

The analysis presented here was performed under a U.S. Department of Energy contract with Bechtel Bettis, Inc. The authors wish to acknowledge Mr. David Banas and Mr. J. E. Holliday for their help designing and analyzing the specimen, Dr. J. B. Newman for help in programming the return method, Mr. Greg A. Szkrybalo for administrating the contract with Lehigh University, and Mr. Frank E. Stokes and his staff at Fritz Engineering Laboratory at Lehigh for their careful conducting of these tests. We are also grateful to Ms. Virginia Ogurchak for her help in preparing this document.

References

- [1] "ASME Boiler and Pressure Vessel Code, 1998, Section III, Appendix A, Article A-8000," American Society of Mechanical Engineers.
- [2] Slot, T., 1972, "Stress Analysis of Thick Perforated Plates," Ph.D. Thesis, Dept. of Mech. Engr., The University of Technology Delft, the Netherlands, Technomic Publishing Co., Inc.
- [3] W. D. Reinhardt, 1998, "Yield Criteria for the Elastic Plastic Design of Tubesheets with Triangular Penetration Patterns", PVP Vol. 370, *Finite Element Applications: Linear, Non-Linear, Optimization and Fatigue and Fracture*, pgs. 113-120.
- [4] Reinhardt, W., 1999, "A Fourth-Order Equivalent Solid Model for Tubesheet Plasticity," presented at the 1999 ASME PVP Conference, PVP-Vol. 385, *Computer Technology - 1999*, pgs 151-158.
- [5] J.L. Gordon, Jones, D.P., Banas D., and Hutula, D.N., 1999, "A Collapse Surface for a Perforated Plate with an Equilateral Triangular Array of Penetrations," presented at the 1999 ASME PVP Conference, PVP Vol. 385, *Computer Technology - 1999*, pgs. 125-134.
- [6] D. P. Jones, J. L. Gordon, Hutula, D. N., Banas, D., Newman, J. B., 2001, "An Elastic-Plastic Flow Model for Finite Element Analysis of Perforated Materials," *Transactions of ASME, J. of Pressure Vessel Technology*, Vol. 123, No. 3, pgs. 265-270.
- [7] D. P. Jones and J. L. Gordon, 2001, "Collapse Surfaces for Perforated Plates with Triangular Penetration Patterns for Ligament Efficiencies between 0.05 and 0.50," presented at the 2001 ASME PVP Conference, PVP-Vol. 417, *Emerging Technologies: Advanced Topics in Computational Mechanics and Risk Assessment*, pgs 67-78.
- [8] J. L. Gordon and D. P. Jones, 2002, "Application of a Sixth Order Generalized Stress Function to Determine Limit Loads for Plates with Triangular Penetration Patterns," to be presented at the ASME Pressure Vessels and Piping Conference, B-T-3396, November, 2001.

[9] *ABAQUS: Theory Manual Version 5.8*, 1998, Hibbit, Karlsson & Sorensen, Inc., Farmington Hills, MI.

[10] A. Kalnins and D. P. Updike, 1999, "Limit Analysis of an Autoclave Lock Ring," presented at the 1999 ASME PVP Vol. 383, Conference , PVP-Vol. 383, *Pressure Vessels and Piping Codes and Standards - 1999*, pgs 171-178.

Table 3. Collapse load results.

Method	Material Allowable (psi)	Load (kips)	[Avg of Test]/Calculated
Test 1		2,734	-
Test 2		2,706	-
Explicit FEA	38,030	843	3.24
EPP-EQS UMAT4	38,030	714	3.81
EPP-EQS UMAT6	38,030	738	3.69

Figure 10. Load-Deflection Curves.

